INFLUENCE OF NOISE ON THE STATISTICAL PROPERTIES OF LIDAR SIGNALS DUE TO AEROSOL

Yu.S. Balin, I.A. Razenkov, and A.P. Rostov

Institute of Atmospheric Optics,
Siberian Branch of the Academy of Sciences of the USSR, Tomsk
Received October 2, 1989

Distortions of the coherence and phase spectra of the aerosol lidar returns due to the noise have been studied theoretically and experimentally. An analysis has been carried out for the section of the sounding path considered as a linear system with one input and one output. A formula has been derived that allows one to obtain the unbiased estimate of the wind velocity from the phase spectra of lidar returns mixed with noise.

In sounding the lower troposphere the lidar return is determined, to a great extent, by light scattering on aerosol particles whose concentration varies in time and space.

For this reason a set of spatio–temporal samples of signals recorded with the use of a lidar is also random. At present for the statistical description of the obtained data file the methods of correlation and spectral analysis are widely used for practical implementation of techniques for remote measurements of the parameters of the atmospheric turbulence and the wind velocity.[1,2] The derivation of useful information from the sounding data has brought about the need for estimating the signal distortions of different physical nature. The problems of taking into consideration the main sources of noise, namely, the multiplicative noise due to the fluctuations in the energy of sounding radiation and the additive noise of the lidar recording channel, when performing the correlation analysis, have been described in detail in Ref. 3.

In the present paper the distortions of the statistical characteristics of lidar returns due to the noise are studied using the spectral analysis.

As is well known, the main range of applicability of the spectral analysis in applied problems is studying the input and output processes of the linear systems. The laser sounding can also be treated as a hypothetical linear system with one input and one output.[4] Figure 1 shows this concept schematically, where the section r of the sounding path is isoplanar with the wind velocity vector $\boldsymbol{V}$ and φ is the angle between them. The aerosol inhomogeneities entrained by the wind cross the section r and cause the fluctuations in the lidar signals. We denote a time series of the input signals by $x(t)$ and that of the output signals by $y(t)$. The parameters of the linear system describing the aerosol inhomogeneities transport are characterized by coherence $\gamma(f)$ and phase $\theta(f)$ functions determined from the power spectra of signals measured at the input and output of the system. The coherence function indicates the fraction of the signal power at the frequency f associated with the contribution of the aerosol inhomogeneities crossing this section of the sounding path. The phase angle $\theta(\mathrm{f})$ defines the transit time of an inhomogeneity across the system, i. e., it depends on the spacing r and the wind velocity V:

$$\theta(\mathrm{f}) = -2\pi f r/V. \qquad (1)$$

According to the theory of linear systems, we have for the experimentally recorded processes $x(t)$ and $y(t)$

$$\gamma^2_{xy}(f) = \frac{|G_{xy}(f)|^2}{G_{xx}(f)G_{yy}(f)}\,,\ \Theta_{xy}(f) = \arctan\frac{\mathrm{Im}\ G_{xy}(f)}{\mathrm{Re}\ G_{xy}(f)}\,, \qquad (2)$$

where $G_{xx}(f)$, $G_{yy}(f)$, and $G_{xy}(f)$ are the autospectra and cross–spectrum of the signals $x(t)$ and $y(t)$, respectively.

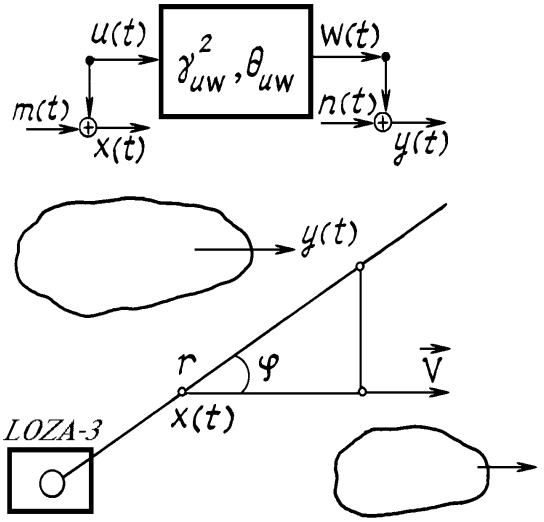

FIG. 1. Diagram showing the idea that the sounding path can be represented as a linear system.

To derive analytical relations demonstrating the effect of noise on the coherence and phase spectra we represent the processes $x(t)$ and $y(t)$ in the form of a sum of the signals $u(t)$ and $w(t)$ and the corresponding noise $m(t)$ and $n(t)$ (Fig. 1):

$$\begin{aligned} x(t) &= u(t) + m(t); \\ y(t) &= w(t) + n(t). \end{aligned} \qquad (3)$$

Although the noise of the reference channel (fluctuations of the sounding pulse energy) enters in the signals multiplicatively, additive representation (3) is valid under certain conditions. One of them are small variations of the components of the process. This condition is easily satisfied since in sounding of the free atmosphere the short–period (5–10 min) variations of the backscattering coefficients

0235-6880/91/04 328-05 $02.00

were less than or equal to 10% (Ref 3) As a rule, the output energy fluctuations of solid–state lasers in this time were about several per cent.[5] One more condition is that the measurement data should be centered preliminary in the course of their mathematical processing.

In our further analysis we will deal with uncorrelated and correlated input $m(t)$ and output $n(t)$ noise as had been the case in Ref. 4. Since in the case of lidar sensing of the atmosphere the inequality $rL^{-1} \ll 1$ is practically always valid, the signal–to–noise ratios at the input and output of the system coincide.

With uncorrelated input and output noise, i.e., when $G_{mn}(f) = 0$, we can write the following relations for the coherence and phase spectra:[4]

$$\gamma^2_{xy}(f) = \gamma^2_{uw}(f)[1 + \alpha(f)]^{-2}; \tag{4}$$

$$\theta_{xy}(f) = \theta_{uw}(f), \tag{5}$$

where $\alpha(f) = G_{mn}(f)/G_{uu}(f) = G_{nn}(f)/G_{ww}(f)$ is the signal–to–noise ratio.

Hence it follows that uncorrelated noise in the lidar returns leads to a decay of the coherence spectrum but does not affect the phase angle. The latter means that the wind velocity estimated from the phase spectrum is unbiased.

Let us now consider the case when noise $m(t)$ and $n(t)$ are correlated (laser energy fluctuations), i.e., when $G_{mn}(f) \neq 0$. The formula for the cross–spectrum $G_{xy}(f)$ is then written in the form

$$G_{xy}(f) = G_{uw}(f) + G_{nm}(f). \tag{6}$$

Further calculations can be substantially simplified and more vivid if the spectra sought are represented graphically in a complex plane shown in Fig. 2. This figure shows the cross–spectra $G_{uw}(f)$ and $G_{xy}(f)$ in polar coordinates, where the line segments correspond to the moduli of the corresponding spectra and the slope angles – to the phase angles $\theta_{uw}(f)$ and $\theta_{xy}(f)$.

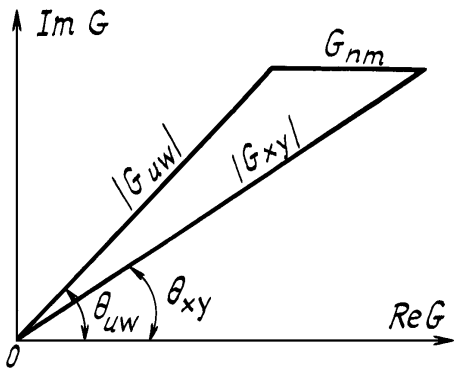

FIG. 2 Diagram of spectra in polar coordinates in the complex plane.

Based on this graphic representation, Bendat and Pirsol considered two particular cases, when $|G_{mn}(f)|$ is parallel to $|G_{uw}(f)|$ and $|G_{mn}(f)|$ is perpendicular to $|G_{uw}(f)|$. As $\gamma^2_{mn} = (f) \to 1$ for the first variant, when $\theta_{xy}(f) = \theta_{uw}(f)$ and the minimum of the coherence function is equal to

$$\gamma^2_{xy}(f) = \{[1 - \alpha(f)]/[1 + \alpha(f)]\}^2. \tag{7}$$

For the second variant, when $\theta_{xy}(f) = \theta_{uw}(f) + \Delta\theta_{mn}(f)$, we have[4]

$$\gamma^2_{xy}(f) = [1 + \alpha^2(f)]/[1 + \alpha(f)]^2 \tag{8}$$

In our case since the noise fluctuations at different points of the path are synchronous, the modulus $|G_{mn}(f)|$ is parallel to the real axis. Then for the coherence and phase functions we can derive the following formulas:

$$\gamma^2_{xy}(f) = \frac{\gamma^2_{uw}(f) + 2\alpha(f)\gamma^2_{uw}(f)\cos\theta_{uw}(f) + \alpha^2(f)}{[1 + \alpha(f)]^2}, \tag{9}$$

$$\theta_{xy}(f) = \arctan \frac{\sin\theta_{uw}(f)}{\cos\theta_{uw} + \alpha(f)\,\gamma^{-1}_{uw}(f)}. \tag{10}$$

As can be seen from Eqs. (9) and (10), the coherence and phase spectra derived from the experimental data in the existence of a correlated noise on the sounding path are always distorted. The degree of distortion is determined from the signal–to–noise ratio $\alpha(f)$, therefore it is natural to expect that the least distortions of the spectrum occur at low frequencies where the ratio $\alpha(f)$ is minimum because of the power–law character of the valid signal spectrum.[1,6,7] It should be noted that in contrast to the case of uncorrelated noise, the phase spectrum here experiences noise distortions. Nevertheless, it follows from Eq. (10) that for the phase angles being multiple of π, the angle $\theta_{xy}(f)$ measured experimentally should coincide with its true value $\theta_{uw}(f)$. This conclusion can easily be supported graphically in Fig. 2. It is clear that with increase of frequency the line segment corresponding to $G_{xy}(f)$ must rotate about the origin of the coordinate system. When the angle $\theta_{xy}(f)$ reaches the value $\pm\pi$, all line segments corresponding to the spectra $G_{xy}(f)$ become parallel to the abscissa. This, in turn, means that the phase angles $\theta_{uw}(f)$ and $\theta_{xy}(f)$ coincide. The latter, according to Eq. (1), allows us to obtain a simple formula for an unbiased estimate of the wind velocity.

$$V = -2f_\pi r\cos\varphi,$$

where f_π is the frequency at which the phase reaches $\pm\pi$.

The experimental studies of the statistical properties of lidar returns were carried out using a *LOZA 3* lidar in August–September, 1988 near Tomsk over a flat underlying surface. The sounding path was located at an elevation angle 3–5° in the direction along the wind velocity. The recording system of the lidar enabled us to record the lidar return with the 20 m step along the sounding path. The first strobe was taken at an altitude of 10 m and the last – at an altitude of 30 m.

Two horizontal components of the wind velocity were measured simultaneously at a frequency of 4 Hz using an acoustic anemometer[9] placed on the meteomust at an altitude of 20 m corresponding to the middle point of the measuring section of the lidar path. The rate of the lidar readings in the formation of temporal series of signals was equal to 2 Hz. The lidar and anemometer data were synchronously recorded on an Elektronika–60 microcomputer and the period of observation was 30 min. The modulus and the direction of the average

wind velocity as well as the data on wind velocity fluctuations were obtained using the anemometer. The auto– and cross–spectra of lidar returns were calculated from lidar data using the fast Fourier transform.[4,6] To increase the reliability of the statistical data, the spectra were averaged over the ensemble obtained in processing of the lidar data corresponding to the different pairs of points along the sounding path.[6,7] The coherence $\gamma^2_{xy}(f)$ and phase $\theta_{xy}(f)$ spectra were found from the spectra of lidar returns using formulas (2).

Actual spectra $\gamma^2_{xy}(f)$ and $\theta_{u\tilde{w}}(f)$ were calculated using the anemometric data on the absolute value of the wind velocity, direction, and fluctuations based on the theory described in Ref. 7. In the calculations we accepted the hypothesis of the "frozen" turbulence since the lidar readings were closely spaced while the lifetime of the inhomogeneities is about several tens of seconds.[3,7] This means that during the time of propagation of the aerosol inhomogeneities between the points of measurements on the path their shapes change insignificantly.

On the whole, 27 series of measurement were statistically processed. In two cases we failed to derive the desired information from lidar data since the variations of the signals were less than 2%, and the signal–to–noise ratio was smaller than unity.

As an illustration, Figs. 3 and 4 show the typical coherence and phase spectra derived from two successive realizations under stable meteorological conditions on September 5, 1988. The acoustic anemometric measurements gave the average wind velocity of 3.8 and 3.9 m/s, respectively, and the value of the wind velocity fluctuations about 11% in both cases. The lidar data are denoted by circles and the theoretical calculations of the coherence and phase functions are shown by curves *2–5*. The confidence intervals corresponded to the number of degrees of freedom $n = 128$ when the significance level was taken to be 0.05.

In processing the experimental data the coherent and incoherent components of the noise were separated. The separation was carried out using the technique presented in Ref. 10 on the basis of the analysis of the values of discontinuities of auto– and cross–correlation functions with zero delays. The signal–to–noise ratios were equal to 32 and 10 for uncorrelated noise and 49 and 12 for correlated noise in the first (Fig. 3a) and second (Fig. 3b) realizations, respectively. The total ratio of variances of the SNR for the data shown in the upper part of the figure was equal to 19 and in the second case it was equal to 6. The frequency dependences $\alpha(f)$ obtained taking into account the power–law character of the spectrum $G_{uu}(f)$ of the valid signal are shown in Fig. 3 by curves *1*.

True values of $\gamma^2_{u\tilde{w}}(f)$ and $\theta_{u\tilde{w}}(f)$ are shown in the figures by curves *2*. The effect of uncorrelated noise on the general behavior of the dependences $\gamma(f)$ (curves *3* in Fig. 3) calculated according to Eq. (4) is weak. It merely reduces the coherence spectrum. Since the uncorrelated noise does not influence the phase angle there are no such dependences in Fig. 4.

The existence of the coherent noise in the reference channel leads to significant distortions of the coherence and phase spectra at the middle and high ($f > 0.1$ Hz) frequencies. The calculated results based on relations (9) and (10) are shown in Figs. 3 and 4 by curves *4*.

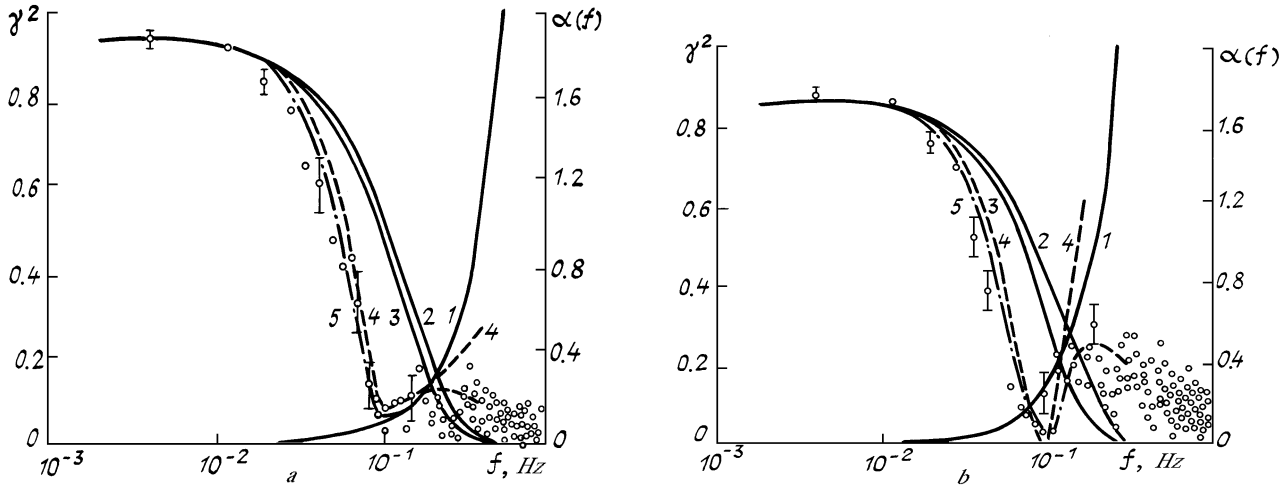

FIG. 3. Comparison between the theoretical and experimental coherence functions with different sources of noise for different signal–to–noise ratio: a) SNR = 19; b) SNR = 6. Curve 1 shows $\alpha(f)$, curves 2–5 show theoretical calculations of $\gamma^2(f)$ and circles show the experimental results.

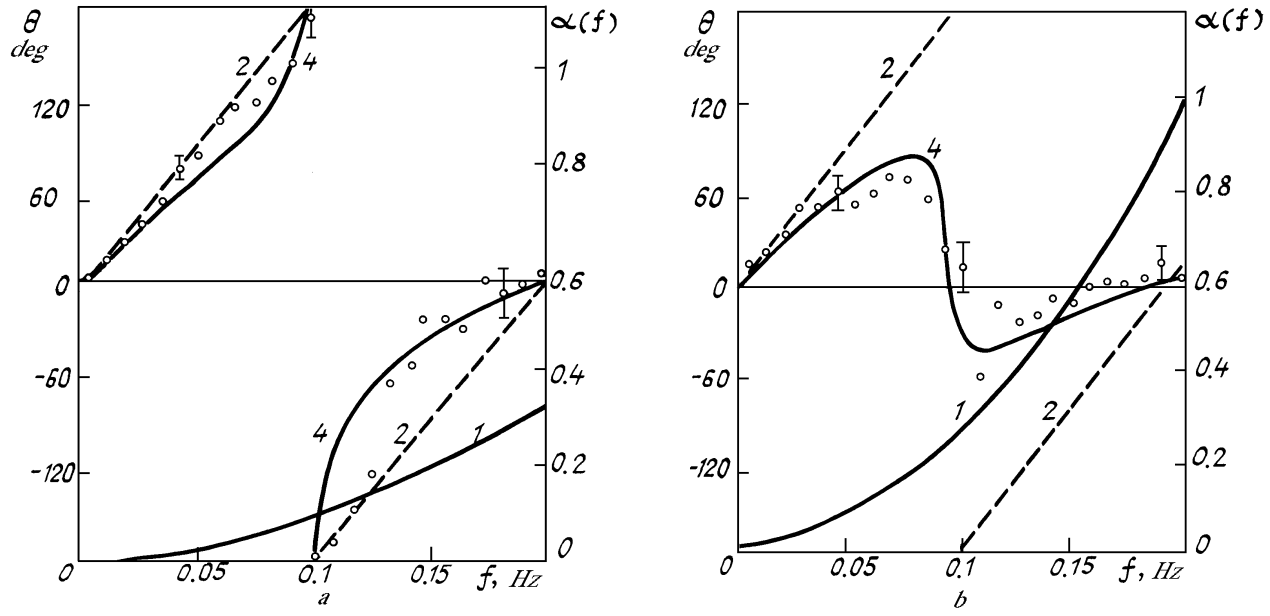

FIG. 4. Comparison between the theoretical and experimental functions of the phase angle. Initial data are identical to Fig. 3. Curve 1 shows α(f), curves 2 and 4 show the theoretical calculation of θ(f), and circles show the experimental data.

In the low– and middle frequency ranges the effect of correlated noise appeared in the decrease of the absolute values of the coherence and phase spectra. The experimental data in this case were in satisfactory agreement with the theoretical results. In the high–frequency range the coherence spectrum rose. This is explained by the predominant effect of the coherent noise. As can be seen from the figure, in this frequency range the rate of growth of the coherence function increased with increase of the signal–to–noise ratio. At the same time, at $f > 0.1$ Hz the curves and the experimental data on $\gamma^2_{xy}(f)$ differ strongly. At first the values $\gamma^2_{xy}(f)$ increase and then they tend to decrease. On the whole, in this part of the figure the values of the coherence spectra are concentrated near $\gamma^2_{xy}(f) = 0.1–0.2$.

Such disagreement between the calculations and experiment can obviously be explained by simultaneous effect of two factors. The correlated noise, when it becomes predominant, results in the increase of the degree of coherence while the uncorrelated noise always leads to its decrease. The rigorous consideration of the simultaneous effect of these factors seems to be difficult. Nevertheless, if we assume the influence of both types of noise be independent, then $\gamma^2_{xy}(f) = \gamma^2_{uw}(f) K_c(f) K_u(f)$. Here $K_c(f)$ and $K_u(f)$ are functions of frequency ($K_c(f)$, $K_u(f) < 1$) that distort the degree of coherence due to the correlated and uncorrelated noise, respectively.

The formula for calculating $\gamma^2_{cxy}(f)$ with an account for the simultaneous effect of these factors takes then the form

$$\gamma^2_{jxy}(f) = \frac{\gamma^2_{cxy}(f)\,\gamma^2_{uxy}(f)}{\gamma^2_{uw}(f)}, \qquad (11)$$

where $\gamma^2_{cxy}(f)$ and $\gamma^2_{uxy}(f)$ are the coherence functions obtained with an account for the effect of the correlated (curve *2*) and uncorrelated (curve *3*) noise, respectively.

The calculated results for $\gamma^2_{cxy}(f)$ shown in Fig. 3 by curve *5* agree with the experimental data best of all. This allows us to assume that this approach is justified.

The effect of noise on the phase spectra was weak but their shapes differ substantially depending on the signal–to–noise ratio. When $\alpha(f)$ increases (Fig. 4b), a substantial deformation is observed in the spectrum at middle frequencies. However, according to the aforementioned conclusion, the noise has no effect on the true value of the phase spectrum at $f = f_\pi$. As can be seen from Fig. 4a, curves *2* and *4* are intersected at this point. When the signal–to–noise ratio decreases (Fig. 4b), curve *4* intersects the abscissa. It should be noted, however, that in the last case the determination of f_π is impeded by a large statistical error because of the small value of the coherence spectrum $\gamma^2_{xy}(f_\pi)$. This difficulty can be overcome by calculating the phase spectrum for increased spacing r between the measurement points along the sounding path. This means that the lidar system is adjusted to larger scale of the aerosol inhomogeneities and, hence, we shift toward the lower frequencies of the spectrum where the signal–to–noise ratio is higher. The shape of the phase spectrum becomes similar to that of the spectrum shown in the left part of the figure. It is natural in this case that the error in determining the position of f_π increases, because of the discrete character of the measured spectra since the increment of the value Δf is determined by the realization length.

Thus for the lidar facilities used and for the aerosol inhomogeneities of the size normally occurring in the atmosphere and the moderate winds, the use of the spectral analysis to process statistically the lidar data is limited by the frequency range f below ~ 0.1 Hz.

REFERENCES

1. E.W. Eloranta, J.M. King, and J.A. Weinman, Appl. Meteor., No. 14, 1485–1489 (1975).

2. E.D. Hinkley, ed. , *Laser Monitoring of the Atmosphere* [Russian translation] (Mir, Moscow, 1979), 416 pp
3. G.G. Matvienko, G.O. Zadde, E.S. Ferdinandov, et al. *Correlation Methods of Laser Sounding of the Wind Velocity* (Nauka, Novosibirsk, 1985), 220 pp.
4. J. Bendat and A. Pirsol, *Applications of Correlation and Spectral Analysis* [Russian translation] (Mir, Moscow, 1983), 312 pp.
5. Yu.F. Arshinov, Yu.S. Balin, et al. , Kvantovaya Elektron. **10**, No. 2, 390–397 (1983).
6. Yu.S. Balin, M.S. Belen'kii, I.A. Razenkov, and N.V. Safonova, Opt. Atm. **1**, No. 8, 77–83 (1988).
7. Yu.S. Balin, M.S. Belen'kii, et al. , Izv. Akad. Nauk SSSR Ser. Fiz. Atmos. Okeana **22**, No. 10, 1060–1063 (1986).
8. Yu.S. Balin, G.S. Bairashin, V.V. Burkov, et al. , in: *Problem–Oriented Measurement–Calculating Complexes* (Nauka, Novosibirsk, 1986), pp. 65–71.
9. M.V. Anisimov, E.A. Monastyrnyi, G.Ya. Patrushev, and A.P. Rostov, Prib. Tekh. Eksp. No. 4, 196–199 (1988).
10. R.L. Kagan and L.S. Gandin, *Statistical Methods in the Interpretation of the Meteorological Data* (Gidrometeoizdat, Leningrad, 1976), 359 pp.